



## Shear Behavior of Reinforced Beam Cast with Super Crete (Icon)

Salah A Aly<sup>1</sup>, Mohammed E Issa<sup>2</sup> and Magda M Elgaml<sup>3</sup>

<sup>1</sup>Department of Reinforced Concrete Structures,

Housing and Building National Research Center (HBNRC), Cairo, Egypt

<sup>2</sup>Department of Reinforced Concrete Structures at Faculty of Engineering, Cairo University, Cairo, Egypt

<sup>3</sup>Department of Civil Engineering Department, Faculty of Engineering, Cairo University, Cairo, Egypt  
salahaly62@gmail.com

### ABSTRACT

The Super Crete (Icon) is one of the polymer concrete types that was developed recently in many countries and still considered as a new material especially in Egypt. It is a concrete without coarse aggregate that consists of powder material (which contains high percentage of calcium silicate) and polymer liquid. So it looks like a mortar paste more than a concrete. The use of powder material and polymer liquid for the production of new type of concrete is one common means for achieving a more environment-friendly concrete. Icon has shown superior high performance in compressive strength, durability, very fast curing time and very low permeability that breaks the current known limitations. It has been used widely in the architectural applications like decorative features, facade and cladding. Due to the newness of Icon and the lack of information about the materials and manufacturing process of this type in the Egyptian market, this research was carried out to investigate the shear behavior of polymer concrete beams under different conditions. The shear strength is one of the important properties of concrete polymers when used in structural elements subjected to shear like slender beams and columns. Fifteen beams were cast to investigate the effect of the shear span to depth ratios, different locations and different reinforcement of openings on the shear behavior of the tested specimens. All these beams were designed to fail in shear. The test results showed that, the absence of coarse aggregates reduced the ultimate shear strength of the fine aggregate polymer concrete. This may be attributed that, the rougher crack surfaces are better able to transfer shear due to aggregate interlock. The validity of both the Egyptian Code for the design and implementation of Concrete Structures (ECCS) 203-2007 and American Concrete Institute (ACI) 318-2011 Codes for estimating the shear strength of the tested Super Crete beams was investigated. The research described in this paper provides additional experimental information on the shear behavior of polymer concrete beams. Different conclusions and recommendations are introduced.

**Key words:** Polymer concrete, shear strength, shear span and openings

### INTRODUCTION

Recently and due to the leakage of natural coarse aggregates, it has been become a necessary to find an alternative to the convention concrete. Polymer concrete is an example of a relatively new high performance composite material that has been commercialized since the early sixties. The Super Crete (Icon) is one of the polymer concrete types that was developed recently in many countries and still considered as a new material especially in Egypt. This material has many advantages such as very good durability, very low permeability and very fast curing time. Some of the literature studies consider the environmental benefits of polymer concrete, such as the immobilization of toxic metals, while others report on the mechanism of the geo-polymerization process for many different aluminium-silicate minerals. However there are currently very few published studies on the engineering properties. Shear strength is one of the important properties of Icon when used in beams as a structural element. Based on the literature studies, especially when shear span to depth ratio is greater than 2.0, It had to be noted that the shear force in a cracked section is mainly resisted as follows: 20 to 40% by un-cracked concrete of compression zone; 33 to 50% by interlocking action of aggregates across the crack surface; and 15 to 25% by dowel action. It well known that the rougher crack surfaces, which produce by the coarse aggregates, are better able to transfer shear due to aggregate interlock [2]. So, it is very important to investigate the shear behaviour of non-coarse aggregate super Crete. In this research, an experimental study was carried out to investigate the shear behaviour of polymer concrete beams under different conditions.

## RESEARCH SIGNIFICANCE

The aim of the present study is to:

- Investigate the applicability of using The Super Crete (Icon) to produce structural elements.
- Evaluate the effect of the shear span to depth ratios and openings with different locations and reinforcement on the shear behaviour of the tested specimens.
- Assess of the adequacy of the Egyptian ECCS 203-2007 and ACI 318-2011 Codes provisions for predicting the shear strength of the tested Super Crete beam.

## EXPERIMENTAL PROGRAM

### Properties of Material – Concrete Mix

**Traditional Normal Strength Concrete:** CEM I 42.5 N complies with the ESS 4756-1 /2007, was used for constructing the traditional normal strength concrete specimens (six beams). The concrete of this specimen was made with normal weight coarse aggregate composed mainly of silica and silicates (quartz), which is referred to a siliceous aggregate concrete [8]. The proposition of the concrete mix were 1 (Portland cement): 3.46 (coarse aggregate): 1.73 (fine aggregate) by weight. The coarse aggregate used was of 20-mm maximum Nominal size. The water cement ratio was 0.35 and the cement content was 350 kg/m<sup>3</sup>. The target 28th day cube strength was 35 MPa.

**Polymer Super Crete (Icon):** The rest specimens (nine beams) were made from polymer super Crete (Icon) which consists of two components (powder of the material which contains high percentage of calcium silicate plus polymer liquid). The polymer liquid was added to clean drinkable fresh water and mixed well with percentage 1 part of liquid to 300 parts of water, then the solution was placed in the ordinary concrete rotating mixer and the powder of polymer concrete was added gradually during mixing process. Mixing continued until the mix started to shine [4]. The percentage of polymer solution to powder by weight was approximately 18%. The target 28th day cube strength was 37 MPa. Super Crete cylinders of 150\*300 mm (diameter\*height) were cast to obtain the stress-strain relationship and modulus of elasticity as shown in Fig.1, while prisms of 150\*150\*750 mm (width\*depth\*length) were cast to obtain the flexural strength from modulus of rupture tests in accordance with ASTM C 78-02. Table 1 shows the chemical composition of the powder material of polymer super Crete (Icon) which has been determined from X-ray Fluorescence Spectroscopy (XRF) and X-ray Diffraction (XRD) [6]. Table 2 shows the properties of both super Crete and the traditional normal strength concrete.

### Properties of Material – Reinforcement

High-yield deformed and mild steel bars meeting the requirements of the Egyptian specification standards ESS 262/2000 were used for main longitudinal bars and ties, respectively. The high-yield deformed bars had a specified yield strength of 420 MPa and ultimate strength of 650 MPa. The mild steel bars had 285 and 425 MPa of yield and ultimate strength, respectively. The elongation was 29 & 11% for mild and high deformed bar, respectively. The longitudinal bottom and top reinforcement of all specimens was 3Ø12 and 2Ø8, respectively. All specimens had the same transverse reinforcement of 5Ø6/m.

Table -1 Chemical Composition of Powder Material of Polymer Super Crete (Icon)

Oxide	SiO <sub>2</sub>	Al <sub>2</sub> O <sub>3</sub>	Fe <sub>2</sub> O <sub>3</sub>	CaO	MgO	Na <sub>2</sub> O	K <sub>2</sub> O	SO <sub>3</sub>	TiO <sub>2</sub>	P <sub>2</sub> O <sub>5</sub>	Loss in Ignition	Total
Contents (%)	83.49	1.42	0.62	8.09	0.51	0.37	0.1	1.67	0.07	0.02	3.18	99.54

### Fabrication

The specimens were cast horizontally in specially designed forms. Electrical resistance strain gauges were fixed and secured to the reinforcing steel at specific locations before the cage was precisely positional in the form. These strain gauges were fixed at different locations; Fig. 1 to measure the internal steel strain inside the specimens during test. The forms were made from timber with smooth surface and coated with oil before casting concrete. The reinforcement cage then placed in their position in the wooden moulds. Concrete was cast immediately after mixing. The specimens were remoulded on the next day, and subjected to moist curing with water started immediately after casting for two weeks, then left in the atmosphere of laboratory until the date of test.

### Instrumentation

The specimens were instrumented with a variety of sensors to measure the strains, deflections, the load and stroke of the testing machine. The deflection of the specimens was measured using five Linear Variable Distance Transducers, LVDT's, with stroke 100 mm which were attached vertically at equal distance between the two supports (on the bottom face of the specimens), to the concrete surface using 8-mm fisher bolts. The steel strains were measured using electrical resistance strain gauge which attached to the bottom longitudinal steel bars and stirrups before casting the concrete. At the point of load application, a 1000 KN compression load cell monitored the applied load. A portable machine instruments data acquisition system is used in capturing data from the electrical

resistance strain gauges and the LVDT's. Because of the long time needed for each specimen in test, one reading per second was recorded. This rate enables to read all events of the test with a suitable number of readings which can be easily analysed. The loads were controlled by servo controller and measured with load cell. A data acquisition system connected to a personal computer recorded all of the instrumentation readings. The formation and propagation of cracks at different locations were also marked and recorded.

**Table 2: Test Specimens, Concrete Strength, Cracking Loads, and Ultimate Loads**

Group	Beam	Designation	fcu (MPa)	Pu (KN)	δu (mm)
G1	B1	Ref. - 1	38	288	20
	B2	1	39	200	9.9
	B3	Ref. - 1.5	38.5	179	16
	B4	1.5	38	126	5.7
	B5	Ref. - 2	37	155	8.0
	B6	2	41	110	5.4
G2	B7	Ref. - 2	43	147	6.5
	B8	2	45	104	7.0
	B9	Ref. - 2	44	139	7.0
	B10	2	47	98	12
G3	B11	Ref. - 2	42	133	6.8
	B12	2	47	100	5.1
	B13	2	43	124	10.1
	B14	2	45	125	4.3
	B15	2	45.5	140	5.7

Pcr = Cracking load & δu = Deflection corresponding to ultimate load & Pu = Ultimate load & fcu = Concrete compressive strength obtained from testing 150\*150\*150 mm cube

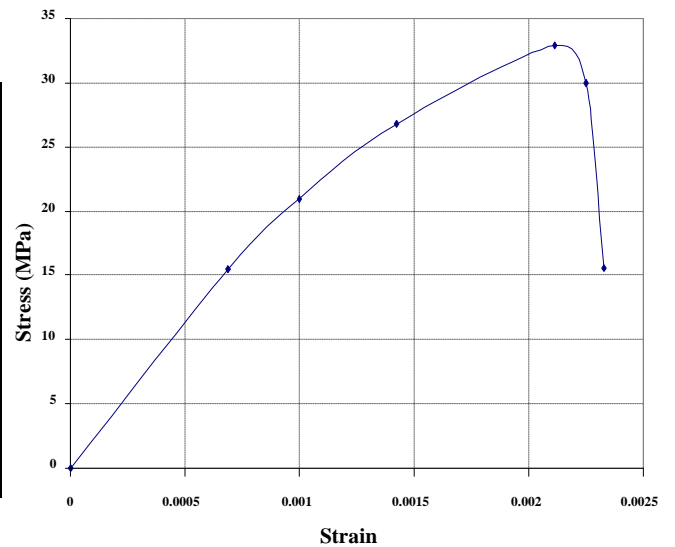
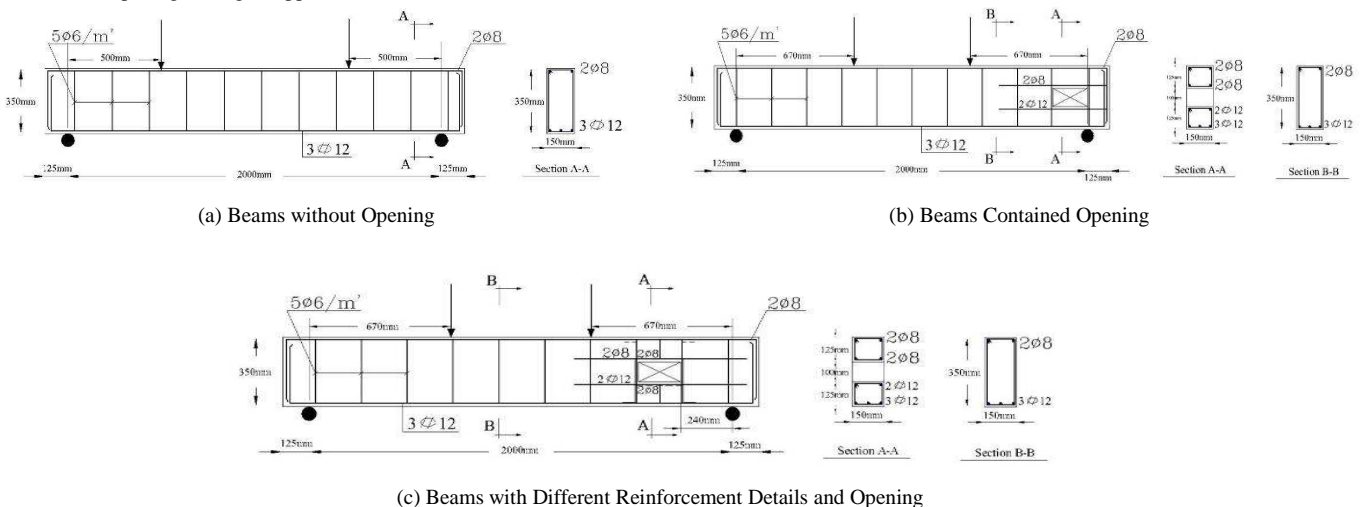


Fig. 1 Stress-Strain Relationships for the Polymer Super Crete (Icon)

**Table -3 Details of the Tested Specimens**

Group	Beam	Designation	a (mm)	d (mm)	a/d	Duct opening	
						As(long)	x (mm)
G1	B1	Ref. - 1	340	340	1	-	-
	B2	1	340	340	1	-	-
	B3	Ref. - 1.5	500	340	1.5	-	-
	B4	1.5	500	340	1.5	-	-
	B5	Ref. - 2	670	340	2	-	-
	B6	2	670	340	2	-	-
G2	B7	Ref. - 2	670	340	2	2Ø12	0
	B8	2	670	340	2	2Ø12	0
	B9	Ref. - 2	670	340	2	2Ø12	470
	B10	2	670	340	2	2Ø12	470
G3	B11	Ref. - 2	670	340	2	2Ø12	240
	B12	2	670	340	2	2Ø12	240
	B13	2	670	340	2	2Ø12	240
	B14	2	670	340	2	2Ø12	240
	B15	2	670	340	2	Pl. 4mm	240

a = Shear span & d = Effective Beam depth & As (long) = Longitudinal steel & x = The distance between the external face of rectangular duct opening and right support.



(c) Beams with Different Reinforcement Details and Opening

**Fig. 2 Details of the Tested Specimens**

### Test Specimens

The experimental work consisted of fifteen beams with the same dimensions, longitudinal and transverse reinforcement. All specimens were designed to experience shear mode failure ensuring that the theoretical flexural strength is considerably higher than the expected experimental shear load. The loading systems were the same in all specimens, but with variable shear span. All specimens had rectangular cross section of 150 mm width and 350 mm thickness, a total length of 2250 mm and were simply supported with a span length of 2000 mm, as shown in fig.2. The longitudinal bottom and top reinforcement of all specimens was  $3\text{Ø}12$  and  $2\text{Ø}8$ , respectively. All specimens had the same transverse reinforcement of  $5\text{Ø}6/\text{m}$ .

The tested specimens were divided into three groups (G1 to G3) depending on the studied parameters. The first group was designed to study the effect of shear span ( $a/d=1, 1.5$  and  $2$ ). The second and third groups were designed to study the effect of location of opening and reinforcement configuration around the opening, respectively. The details of the tested specimens for the three groups were illustrated in table 3 and fig.2.

### Test setup and Procedure

All beams were tested until failure under monotonic increasing static load using a hydraulic actuator of 1000 KN capacity to measure its maximum load capacity. The beams were positioned under the actuator that was mounted on a steel reaction frame. Fig. 3 shows the Test Setup. The hydraulic actuator, load cell and the control vertical LVDT were positioned at the mid-span section. Three different loading types were used according the studied parameters. A very rigid steel beam and neoprene pads were used to distribute the load on the top surface of the beam. The test specimens were simply supported beams with 2000 mm span. The beams were tested with a monotonic increasing load (two point loads) until complete failure took place. The locations of loading points were variable, depending on the shear span of each group. After each load increment, strain readings, deflections and the load were recorded and any visible cracks were marked. The loads were controlled by servo controller and measured with load cell. Fig. 4 shows Schematic of Test Procedure.

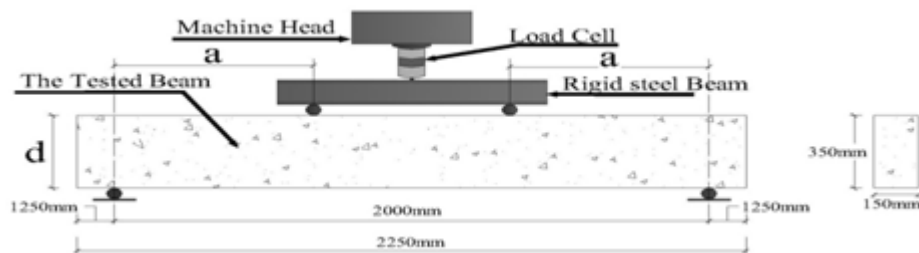


Fig. 3 Test Setup

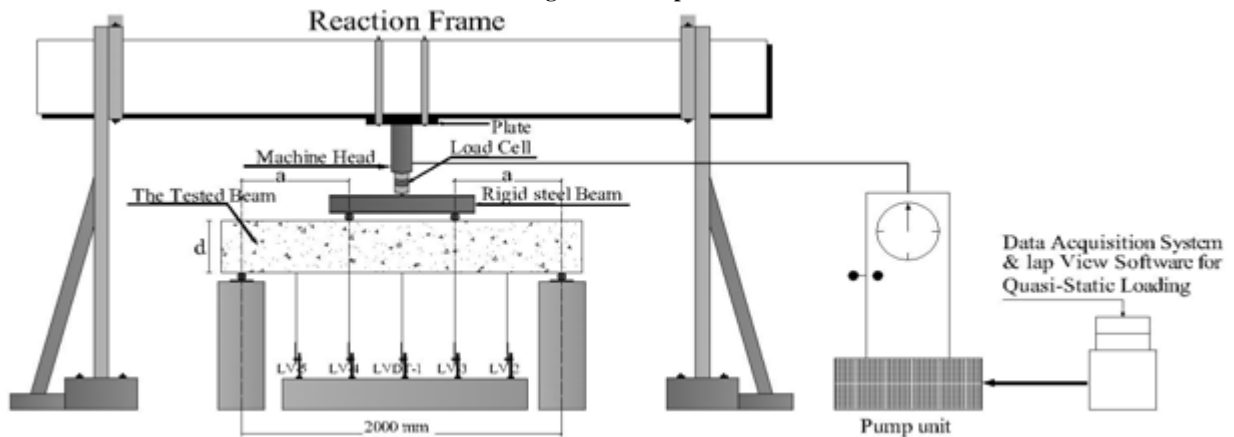


Fig. 4 Schematic of Test Procedure

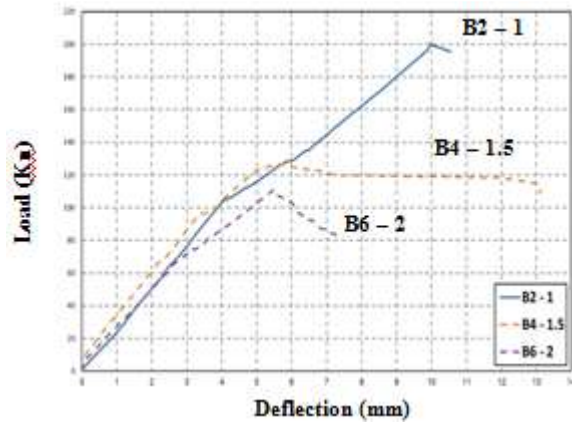
## EXPERIMENTAL RESULTS

The test results of the specimens are summarized in Table -2, in which the beam characteristics, variable parameters, concrete compressive strength, cracking loads, ultimate loads and corresponding deflections are given for each beam.

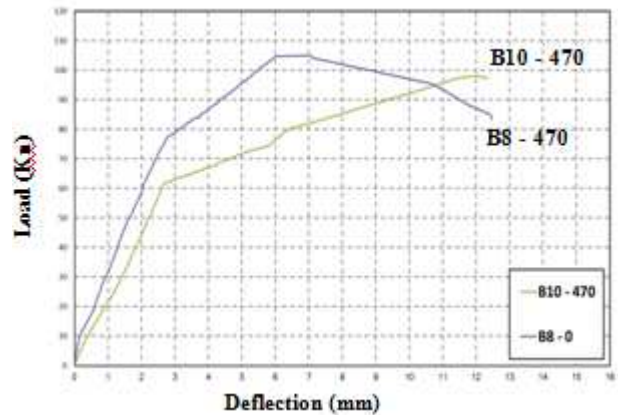
### Load-Deflection Relationship

Table 2 shows the maximum central deflections of all the test specimens at their failure load. Fig. 5 (a) through (c) show the load mid-span deflection relationships of the test specimens. As shown in Fig. 5, the load-deflection relationship is approximately linear till the first yielding of the transverse reinforcement, then the relationship follows a curved path till ultimate load. Beyond the ultimate load, the control specimens (the traditional normal

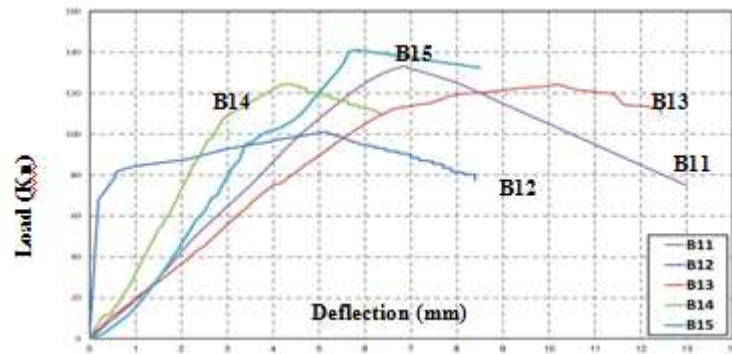
strength concrete specimens) showed gradual and smooth decrease of the load indicating a semi-ductile behaviour. On the other hand, the rest specimens (the polymer super Crete specimens) showed rapid and steep decrease of the load indicating a brittle behaviour. Some specimens retained a part of their capacities while sustaining medium to large plastic deformations. This indicates that these specimens had a stable load-deflection response with large area under the curve and can be classified as semi-ductile behaviour specimens. The corresponding deflection profiles at the ultimate failure load of the tested specimens are shown in Fig. 6 (a-b).



(5-a) Effect of the Shear Span for the Super Crete Beams

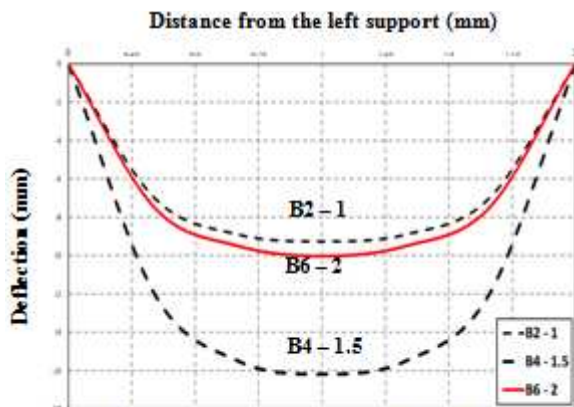


(5-b) Effect of the Location of Opening for Super Crete Beams

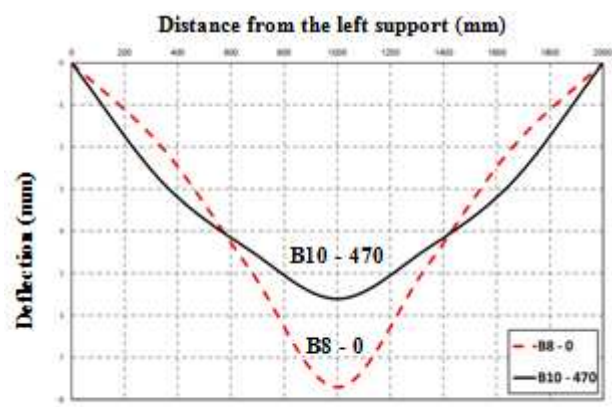


(5-c) Effect of Different Reinforcement Details around Openings

Fig. (5) Load- Deflection Relationship for (a) Effect of the Shear Span for the Super Crete Beams, (b) Effect of the Location of Opening for Super Crete Beams and (c) Effect of Different Reinforcement Details around Openings



(6-a) Effect of the Shear Span for the Super Crete Beams



(6-b) Effect of the Location of Opening for Super Crete Beams

Fig. (6) Deflection Profiles at the Ultimate Failure Load of the Tested Specimens

**Strains in Concrete and Steel Reinforcement**

In most specimens, failure took place without much of a descending branch in the load-deflection curves. The lack of descending branch behaviour in the load-deflection curves implies that these beams may have failed prior to the development of any significant strain localization. Fig. 7 (a-d) shows the load-transverse steel strain relationships for the test specimens. The results suggest that the stress in steel stirrups increased until the steel reaches its yield point.

Thereafter, a large portion of any extra stress is absorbed by large deformations in the steel, which lowers the increase of concrete compressive strain. Before yield, the strain distribution did not vary significantly throughout the length of the test region. With increasing deformation, the strains started to increase considerably at one section or part of the beam while the strains at other sections either remained constant or increased slightly. The strain distribution became more and more non-uniform as failure was approached. In general, higher compressive strains were measured above the location of cracks. As can be seen from Fig. 8 (a) through (d), the strain measured on the longitudinal steel bars at the ultimate load was approximately 0.001. This may be attributed that the longitudinal steel bars didn't reach yield strain before crushing of the concrete. At the ultimate load, the strain measured on the transverse steel bars (stirrups) was approximately 0.0025 and the diagonal concrete strain was about 0.003.

**Cracking Behaviour and Failure Modes**

Fig. 9 (a) through (e) shows the failure modes of all the tested specimens. At early stages of loading, flexural vertical cracks appeared at the beam bottom side, then diagonal tension shear crack appeared suddenly and the load dropped. The diagonal tension crack started horizontally close to the support due to bond slip of bottom reinforcement, and then the crack became diagonal and extended to the point of load application at the beam top side. Similar characteristics were noticed for the cracking patterns of the test specimens. Upon increasing the load, the number, width and extensions of the cracks were increased. After the complete formation of the diagonal crack, brittle failure occurred. This may be attributed to the presence of shear reinforcement, which restrict the growth of diagonal cracks and reduces their penetration into the compression zone; and hence increases the part of the shear force resisted by the concrete compression zone. In addition, the presence of stirrups enhanced the dowel action. The diagonal crack width was observed and the maximum load carrying capacity was recorded. For all beams, once the primary diagonal crack extended to the point of load application and to the support or near the support, the beams failed and the shear dominates the failure mode of all beam specimens. The failure was localized at a section where a primary diagonal crack existed. The branches of adjacent primary cracks connected to form a failure plane with crushing at a section.

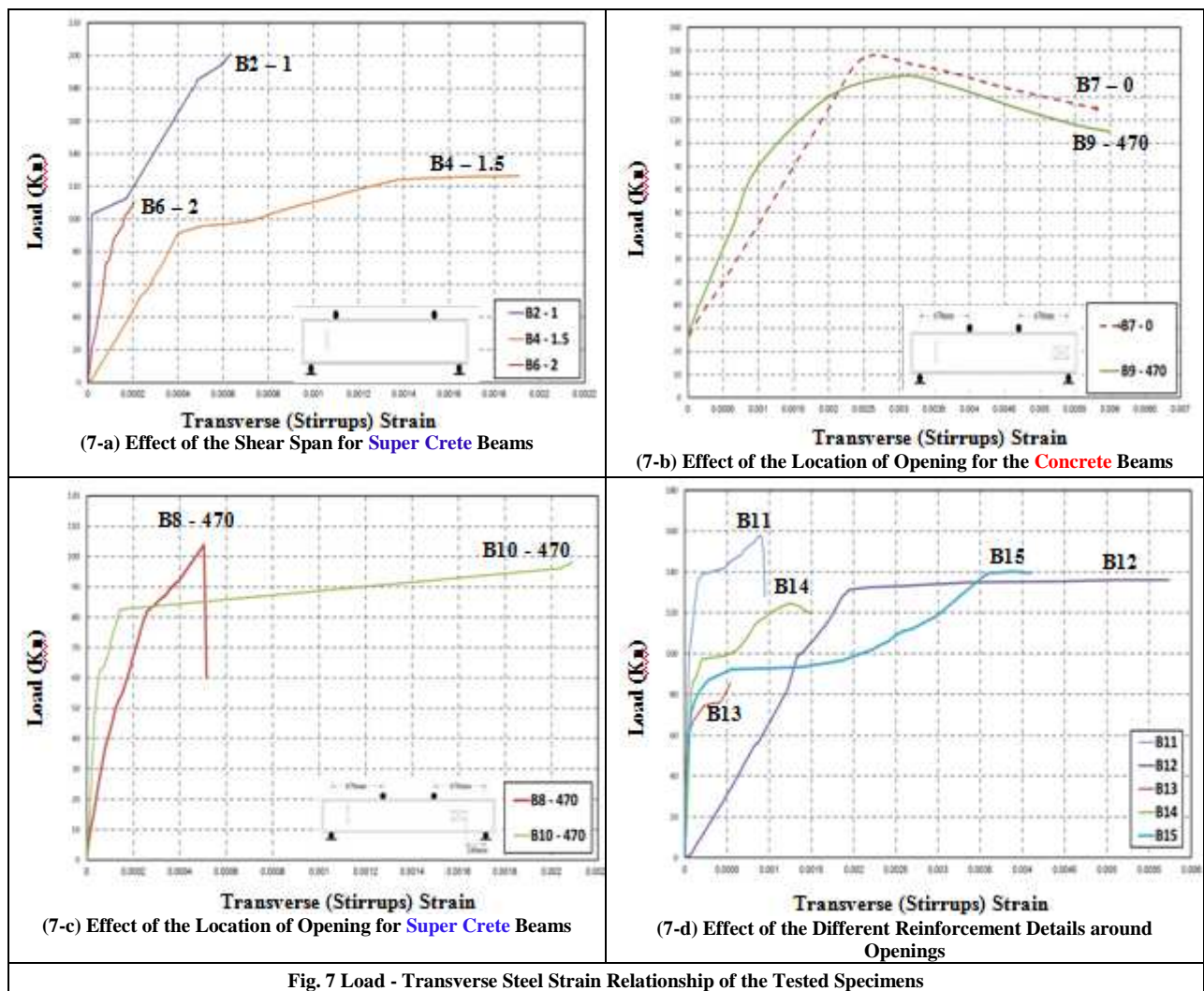


Fig. 7 Load - Transverse Steel Strain Relationship of the Tested Specimens

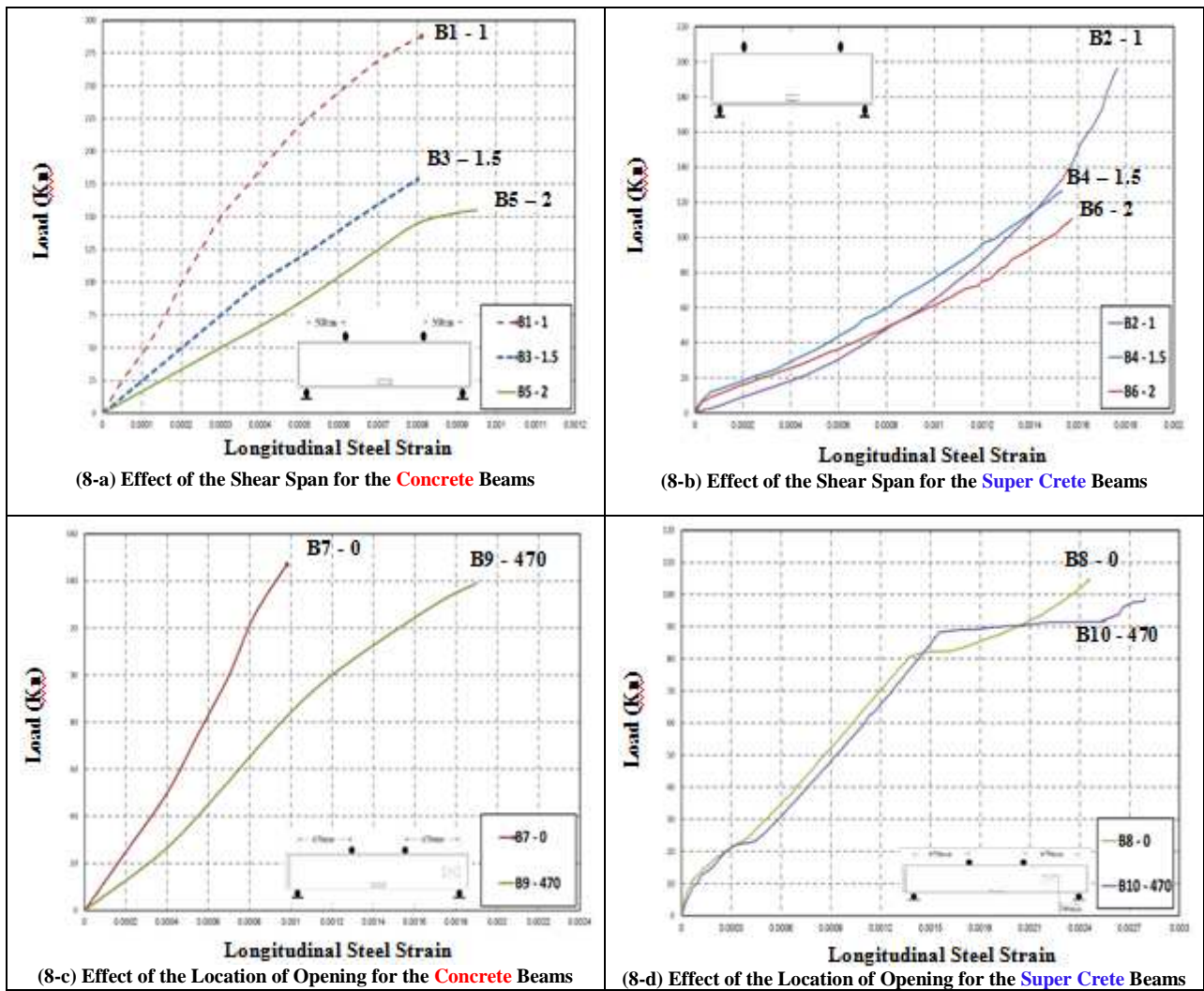
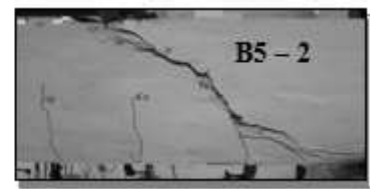
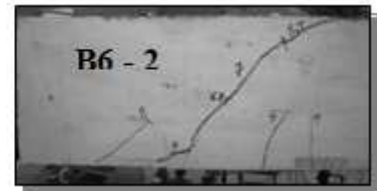


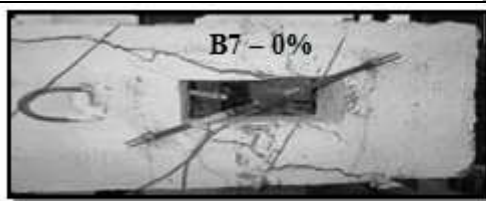
Fig. 8 Load - Longitudinal Steel Strain Relationship of the Tested Specimens



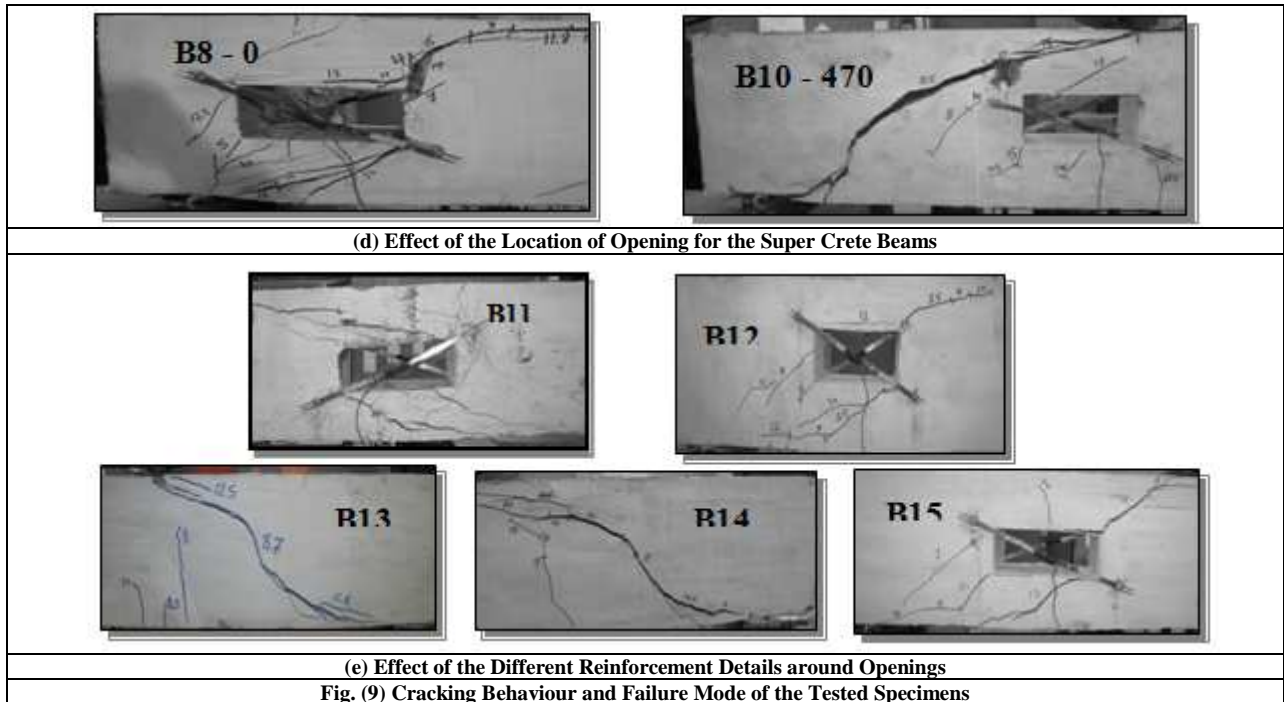
(a) Effect of the Shear Span for the Concrete Beams



(b) Effect of the Shear Span for the Super Crete Beams



(c) Effect of the Location of Opening for the Concrete Beams



## DISCUSSION OF TEST RESULTS

### Effect of Super Crete (Icon)

It can be seen from table 2 and Fig. 5 that the ultimate shear capacity of the Super Crete specimens is lower than those of the traditional reinforced concrete by about 30%. Beams B2, B4, B6, B8, B10 and B12 compared with B1, B3, B5, B7, B9 and B11, respectively.

#### 1. on Deflection

As can be seen from Figs 5 and 6, the Super Crete had a minimal effect on the deflection of the tested beams at the early stages of loading. However, the Super Crete specimens recorded lower inelastic deflections at failure. Beams B2, B4 and B6 compared with B1, B3, and B5, respectively.

#### 2. on Transverse and Longitudinal Steel Strain

As can be seen from Figs 7 & 8, the test results indicated that the Super Crete specimens recorded lower transverse and longitudinal steel strain.

### Effect of Shear Span to Depth Ratio

#### 1. on Shear Capacity

As can be seen from table 2 and Fig. 5, the ultimate shear load decreases with the increases of shear span to depth ratio. Beams B4 and B6 with higher shear span to depth ratio recorded lower ultimate load at failure compared with B2.

#### 2. on Deflection

It can be seen from Fig. 6 that the shear span to depth ratio had a minimal effect on the deflection of the tested beams at the early stages of loading. However, beam of lower shear span to depth ratio recorded higher inelastic deflection at failure. Beam B2 compared with B4 and B6, respectively.

#### 3. on Transverse and Longitudinal Steel Strain

As can be seen from Figs 7 and 8, the test results indicated that beam with lower shear span to depth ratio recorded higher transverse and longitudinal steel strain, beam B2 compared with beam B6.

### Effect of Different Locations of Openings

#### 1. on shear Capacity

As can be seen from table 2 and Fig. 5, the test results indicated that beam with opening far from the support recorded lower ultimate load, beam B10 compared with beam B8.

#### 2. on Deflection

It can be seen from table 2 and Fig. 6 that the deflection of beams increases as the opening becomes far from support, beam B10 compared with beam B8.

#### 3. on Concrete and Longitudinal Steel Strain

Based on the test results shown in Figs 7 and 8, it can be concluded that the transverse and longitudinal steel strains are higher for beams with nearest opening from the support, beam B10 compared with beam B8.



### Effect of Reinforcement Details around the Opening

Referring to table 2, it can be concluded that the ultimate shear capacity increases due to the better reinforcement around the opening. It can be also concluded that strengthening the opening with steel plate can compensate the reduction in the ultimate shear capacity due to the presence of opening.

#### 1. on Deflection

It can be seen from table 2 that the deflection increases due to strengthening the opening with steel plate, beam B15 compared with beams B14.

#### 2. on Recorded Strain

The test results showed that the transverse strain for beams with strengthening opening was observed to be slightly greater than that of beams with conventional reinforcement around the opening, B15 compared with B11, B13 & B14 as shown in Fig. 7.

### CONCLUSION

Based on the experimental results of the tested specimens, the present study shows that the Super Crete (Icon) can be successfully used as a construction material for structural members subjected to different types of shear loading provided that conducting chemical, physical and mechanical tests to ensure its compliance with acceptable criteria. Within the scope of the present study and range of investigated parameters, the following conclusions can be drawn:

- The weight of Super Crete specimens is lighter than those of traditional reinforced concrete. This may be attributed to the absence of coarse aggregate.
- To use Super Crete on a large scale, the behavior of various structural elements cast using this type of polymer must be verified.
- The cracking widths of the Super Crete specimens are wider than those of the traditional reinforced concrete.
- Beams casted using Super Crete can be used as an alternative to the traditional reinforced concrete taking into account that, the ultimate shear capacity of the Super Crete specimens is lower than those of the traditional reinforced concrete by about 30%. This may be attributed to the rougher crack surface for the traditional reinforced concrete which is better able to transfer shear by aggregate interlocking.
- The increase of shear span-to-depth ratio led to reduction of shear strength.
- Beam of lower shear span to depth ratio recorded higher inelastic deflections at failure.
- Strengthening the opening with steel plate can compensate the reduction in the ultimate shear capacity due to the presence of opening.

### REFERENCES

- [1] ACI Committee 318, American Concrete Institute, Building Code Requirements for Structure Concrete Detroit, Michigan, **2011**.
- [2] Egyptian Code of Practice for Design and Construction of Concrete Structures, *ECCS 203*, **2007**, 110-261.
- [3] BG Fonteboa and FM Abella, Shear Strength of Recycled Concrete Beams, *Journal of Construction and Building Materials*, **2007**, 21, 887-893.
- [4] H Hamd, *Behaviour of Composite Polymer Beams Subjected to Torsional Loads*, MSc Thesis, Department of Civil Engineering, Mataria, Helwan University, **2013**.
- [5] TK Mohamed, Flexural Strength of Reinforced Polymer Concrete Beams, *Civil Engineering Research Magazine CERM*, Faculty of Engineering, Al-Azhar University, **2009**, 31(2), 347-363.
- [6] Salah A Aly, Mohammed A Ibrahim and Mostafa M Khattab, Shear Behaviour of Reinforced Concrete Beams Casted with Recycled Coarse Aggregate, *International Science Index*, New York, USA, **2015**.
- [7] M Sofi, JSJ Van Deventer, PA Mendis and GC Lukey, Engineering Properties of Inorganic Polymer Concrete IPCs, *Cement and Concrete Research*, **2007**, 37, 251-257.
- [8] TK Mohamed, SM Elzeiny and OE El-Salam, Flexural Behaviour of Reinforced Beams Cast by Using Polymer Concrete under the Effect of Fire Load, *Civil Engineering Research Magazine CERM*, Faculty of Engineering, Al-Azhar University, **2009**, 31 (2), 739-764.
- [9] U Tayfun, B Ilker and G Atila, Use of Waste Marble and Recycled Aggregates in Self-Compacting Concrete for Environmental Sustainability, *Journal of Cleaner Production*, **2014**, 84, 691-700.
- [10] YM Hussein, Shear Behaviour of Reinforced Beams Cast by Using Non Coarse Aggregate Polymer Concrete ICON, *Civil Engineering Research Magazine CERM*, Faculty of Engineering, Al-Azhar University, **2009**, 31 (2), 669-697.